Journal of Marine Research, 67, 43–70, 2009

Spatial interactions in the *Macoma balthica* community control biogeochemical fluxes at the sediment-water interface and microbial abundances

by Emma Michaud[1,2,3], Gaston Desrosiers[1], Robert C. Aller[4], Florian Mermillod-Blondin[5], Bjorn Sundby[1,6] and Georges Stora[2]

ABSTRACT

We examined how interactions among the three dominant species of the *Macoma balthica* community in the St-Lawrence estuary influence net biogeochemical fluxes and the composition of the sedimentary bacterial community. We manipulated the biodiversity of the community via combinations of *Macoma balthica, Mya arenaria,* and *Nereis virens* in sediment microcosms containing sieved and homogenized tidal-flat sediment. Each combination was adjusted to similar total biovolumes and *in situ* animal densities. Compared to treatments with single species, which were also adjusted to similar biovolumes and densities, combinations of multiple species changed the fluxes of oxygen, phosphate, ammonium, and nitrate across the sediment-water interface and altered the composition of the microbial community beyond the level predicted by linear addition of the single species effects. Most combinations involved positive interactions that increased net fluxes. Although *N. virens* dominated system behavior, we also observed positive interactions between the two bivalves, and between *N. virens* and *M. balthica.* Weaker interactions, sometimes negative, were observed between *N. virens* and *M. arenaria.* Most effects could be directly linked to total oxic sediment volumes and burrow volumes generated by the different species. *N. virens* had the maximum species-specific burrow volume/biovolume ratio, and its presence maximally impacted fluxes. The principal interactions between species that affect net solute fluxes reflect space occupation, life habit (position, location), and irrigation of burrows. These factors interact with reactive substrate distributions and remineralization patterns to produce particular flux balances. Future studies should include the relationships of biodiversity to spatial scales over which the functional groups are distributed, the volumes actively occupied and irrigated, production rates of burrows, and the depths to which the organisms burrow.

1. Institut des Sciences de la Mer de Rimouski (ISMER), 310 allée des Ursulines, Rimouski (Québec), Canada, G5L 3A1.

2. Laboratoire de Microbiologie, de Géochimie et d'Écologie Marines (LMGEM), Centre d'Océanologie de Marseille (COM), Campus de Luminy, Avenue de Luminy, case 901, 13288 Marseille Cedex 09, France.

3. Present address: Laboratoire des Sciences de l'Environnement Marin (LEMAR), UMR6539 UBO/CNRS/IRD, Institut Universitaire Européen de la Mer (IUEM), Technopole Brest Iroise, 29280 Plouzané, France. ***email: emma.michaud@univ-brest.fr***

4. School of Marine and Atmospheric Sciences, Stony Brook University, Stony Brook, NY 11794-5000, U.S.A.

5. UMR-CNRS 5023, Laboratoire d'Écologie des Hydrosystèmes Fluviaux (LEHF), Université Claude Bernard Lyon 1, 69622 Villeurbanne Cedex, France.

6. Earth & Planetary Sciences, McGill University, 3450 University Street, Montreal (Québec), Canada, H3A 2A7.

1. Introduction

The concern that erosion of biodiversity could alter biogeochemical cycling in shallow marine ecosystems has prompted numerous experimental studies of the role of benthic organisms in processing organic matter and regenerating nutrients (e.g., Emmerson *et al.,* 2001; Waldbusser *et al.,* 2004; Mermillod-Blondin *et al.,* 2005; Ieno *et al.,* 2006; Norling *et al.,* 2007). These studies have typically utilized microcosms and manipulated biodiversity by using single species or combinations of species from a common pool of taxa with different values of biomass or species abundance among treatments.

Many of these studies have noted that relationships between statistical measures of biodiversity and nutrient fluxes across the sediment-water interface are not simple (Solan *et al.,* 2004; Mermillod-Blondin *et al.,* 2005; Norling *et al.,* 2007). They concluded, as have earlier studies, that at least with respect to determinants of net nutrient fluxes, species-specific functional traits such as mode of bioturbation, depth of burrowing, and feeding behavior can be as or more important than diversity *per se* (Norling *et al.,* 2007). Thus, the dominant traits of particular benthic species may contribute to so-called idiosyncratic patterns of an ecosystem function, such as nutrient cycling, with increasing diversity (Emmerson *et al.,* 2001).

Some studies have shown that in addition to species-specific bioturbation traits, interactions among species can contribute to variations in elemental cycling and ecosystem functioning (Cardinale *et al.,* 2002; Mermillod-Blondin *et al.,* 2004). Both positive and negative interactions between benthic functional groups have been documented, and biodiversity may be enhanced or decreased as a result of biogenic habitat modification (e.g., Rhoads and Young, 1970; Woodin, 1978; Schaffner, 1990; Widdicombe *et al.,* 2000). Interactions are also density- and biomass-dependent and may vary in sign (e.g., complementary versus competitive) and strength depending on factors such as the sizes of individuals, population abundances, and life habits (Emmerson and Raffaelli, 2000; Solan and Kennedy, 2000; Loreau and Hector; 2001; Mermillod-Blondin *et al.,* 2005; Ieno *et al.,* 2006). Such community properties and interactions must be taken into account in relating biodiversity and ecosystem function (Hughes and Roughgarden, 2000).

There remains great uncertainty regarding species interactions and corresponding biogenic modifications within sedimentary deposits. Waldbusser *et al.* (2004) and Waldbusser and Marinelli (2006) inferred from field studies that spatial organization between species and their burrows may explain variations in reaction rates. Other field, laboratory, and modeling studies have demonstrated the potential roles of burrow abundance, volume, and burrow spacing (packing structure) in generating time-dependent biogenic transport–reaction geometries and thus major biogeochemical impacts (Aller, 1982; 2001; Gilbert *et al.,* 2003). As an example, Michaud *et al.* (2006) showed that two species belonging to the same bioturbation functional group: biodiffusers, defined based on particle transport characteristics, interacted differently with porewater solutes, producing different sediment–water fluxes of ammonium and phosphate. In this latter study, each species occupied the same total biovolume but with different burrow depth distributions.

In the present study, we have determined experimentally how combinations of three benthic species at a constant total biovolume can influence bacterial characteristics of the sediment and the net fluxes of oxygen (O_2), dissolved organic carbon (DOC), phosphate (PO_4^{3-}), ammonium (NH_4^+), and nitrate (NO_3^-) across the sediment-water interface. The species chosen for study are dominant within the *Macoma balthica* community, a community widely distributed in the coastal zones of the North Atlantic (Rosenberg, 2001). Our primary source of benthos for experimental microcosms was the St Lawrence estuary (Quebec, Canada), where the *M. balthica* community is common. The community is characterized by a low number of species and a high number of individuals (Desrosiers *et al.,* 1984). The three dominant species utilized are: the mollusks *Macoma balthica* (Mb) and *Mya arenaria* (Ma), and the polychaete *Nereis virens* (Nv). The effects of these individual species on benthic fluxes were experimentally examined by Michaud *et al.* (2005; 2006), however, the effects of species interactions on biogeochemical fluxes have not been previously studied. The objectives of the present study were: (i) to determine how the direction and magnitude of solute fluxes are modified as a function of different species combinations at a constant biovolume, (ii) to test if system functioning, as measured by net solute fluxes, is controlled by the dominant traits of the species or by interactions among the species, and (iii) to understand the primary mechanisms by which species mixtures determine flux patterns.

2. Material and methods

a. Sampling site

Sediment and animals were collected in August 2003 on a tidal flat in the "Baie des Ha! Ha!" on the south shore of the St Lawrence estuary, 30 km west of Rimouski, Quebec, Canada (Michaud *et al.,* 2005). The tidal flat is sheltered and oriented toward the northwest. Water temperatures vary between 0°C (winter) and 13°C (summer), and the salinity is nearly constant at 27. The sediment consists predominantly of muddy sand (60% mud, 30% sand) with 10% gravel, the organic matter content is approximately 2%, measured as loss upon ignition (500°C), and the sediment porosity is about 0.6 at the surface (0–1 cm).

Surface sediment (0–1 cm) was passed, using seawater from the site of collection, through a 1-mm mesh to remove macrofauna and larger particles. Specimens of *Macoma balthica* (15 ± 5 mm length), *Mya arenaria* (30 ± 10 mm length) and *Nereis virens* (60 ± 10 mm length) were collected at the same time. These three dominant species occur at high densities, 2600–2900 ind *M. balthica* per m^2, 254–760 ind *M. arenaria* per m^2, 1100–1600 ind *N. virens* per m^2 (Mermillod-Blondin *et al.,* 2003). Other species occur at lower densities, for example, tube-living polychaetes (i.e., *Polydora ciliata* and *Spio filicornis*) and erratic movers (i.e., *Scoloplos armiger*) (Mermillod-Blondin *et al.,* 2003), but they were not studied in this work.

Table 1. Experimental design for testing the effects of interactions among species. Each treatment was run in triplicate. Total biomass and total biovolume were determined at the end of the experiment and are presented as the average of triplicates ± standard deviation.

Treatment	Mb	Ma	Nv	Total biomass (g)	Total biovolume (mL)
Control	0	0	0	0	0
Mb	24	0	0	7.51 ± 1.22	11.17 ± 1.04
Ma	0	6	0	19.90 ± 2.35	12.83 ± 1.25
Nv	0	0	12	6.72 ± 1.19	12.16 ± 1.26
Mb + Ma	12	3	0	11.99 ± 1.56	11.83 ± 0.76
Mb + Nv	12	0	6	9.25 ± 1.96	12 ± 1
Ma + Nv	0	3	6	13.87 ± 1.66	12.16 ± 0.28
Mb+Ma+Nv	8	2	4	11.73 ± 1.92	12 ± 1

b. Microcosms

After sieving, sediment was allowed to settle, homogenized by hand, and added to the microcosms to achieve a sediment depth of 15 cm in PVC core tubes (17 cm long, 10 cm i. d.), and covered with 2 cm of seawater. The microcosms were placed in a thermostated room at the average summer temperature for the region (12 ± 0.5°C) with a 12 h light/12 h dark photoperiod. The overlying water of each microcosm was renewed continuously with water from the St-Lawrence estuary (salinity = 27, temperature = 12 ± 1°C; flow ~ 100 mL min^{-1}). The water flow was kept sufficiently low to avoid resuspension of the sediment. The animals were acclimatized in separate tanks for 12 days before introduction into the microcosms. The animals were not fed during the experiment, because we considered there was sufficient food in the sediment and in the seawater coming from the St Lawrence estuary during the experiment. Other authors did not feed animals during their experiments, sometimes for over three months, and they did not observe changes in the behavior of the invertebrates and/or fluxes (Mermillod-Blondin *et al.,* 2005; Norling *et al.,* 2007).

c. Experimental design

The experimental design consisted of eight treatments (control (C), *M. balthica* (Mb), *M. arenaria* (Ma), *N. virens* (Nv), *M. balthica* + *M. arenaria* (Mb+Ma), *N. virens* + *M. balthica* (Nv+Mb), *N. virens* + *M. arenaria* (Nv+Ma), *N. virens* + *M. balthica* + *M. arenaria* (Nv+Mb+Ma)), with three microcosms per treatment (total of 24 microcosms). We normalized the experiments by using a constant total biovolume (BioV) in each treatment in order to facilitate comparisons between treatments (Table 1), instead of the abundance or biomass per se. Gilbert *et al.* (2007) found a linear relationship between biovolume and the particle biodiffusive coefficient, a measure of bioturbation, which suggests that sediment transport and the space occupied by the organisms are functionally coupled. In addition, biovolume may best reflect overall geometric factors (e.g., burrow radius) which couple to solute transport, as described subsequently. Biovolume (BioV)

was determined by measuring water displacement in a graduated test tube after animals were introduced (Michaud *et al.,* 2005; 2006).

The biovolumes of animals used in our experiment were adjusted to natural densities as observed by Mermillod-Blondin *et al.* (2003), and the corresponding wet biomasses were measured (Table 1). After individuals were introduced into the microcosms, *N. virens* and *M. balthica* burrowed more rapidly into the sediment (<10 min and <30 min, respectively) than did *M. arenaria* (<4 h). The 24 experimental microcosms were randomly distributed into three groups of eight. Each group of eight microcosms was prepared at staggered time intervals of three days, and the experiment lasted a total of 39 days for each group. The complete experiment lasted from August 18 to October 2, 2003.

d. Flux measurements

Initial flux measurements in each microcosm group were measured on day 12 after sediment introduction, following which animals were added. Fluxes were measured again on days 20, 28 and 36 (relative times for each microcosm group).

Fluxes were measured during the dark period to exclude the influence of photosynthesis. The flow of water to the microcosms was stopped before each flux incubation. During flux measurements, microcosms, each enclosing a water column of 2 cm (volume = 157 mL; water residence time ~ 1.5–2 min), were sealed with Plexiglas® lids and connected to an inflatable reservoir filled with seawater. This reservoir was used to replace the water that was removed for flux measurements. To avoid artifacts due to low oxygen levels, the incubation time was set to two hours so that total oxygen depletion was less than 20% (Hall *et al.,* 1996). For each flux series, water samples were collected at 30-minute intervals over the two-hour period. The water column in the cores was not stirred continuously during the incubation. Tests using fluorescein dye as a tracer of water showed that the 2 cm water column was completely mixed during the sampling procedure; however, overlying water was homogenized three times during the two-hour incubation. The oxygen concentration was determined by micro-Winkler titration (Grenz *et al.,* 2000). Ammonia was measured spectrophotometrically (Solozarno, 1969) as adapted by Aminot and Chaussepied (1983). Nitrate and orthophosphate were determined with an autoanalyzer (Alpkem FS III, Perstop analytical) (Strickland and Parsons, 1978). Analytical precisions were 0.02–40 μM and 0.04–2 μM, respectively for nitrate and orthophosphate detection (μM = micromolar). All reagents and standards were prepared in acid-washed glasswares, and standards were prepared with a nutrient-free artificial seawater matrix. DOC concentrations were determined with an analytical precision of 1–5% using a high temperature catalytic oxidation (HTCO) method (Shimadzu 5050 TOC Analyser) with platinum catalyst at 680 degrees and non-dispersive infrared gas analyses method. The carrier gas was ultra-zero air (<1 ppm CO_2). Fluxes were calculated from the slopes of the linear regressions of oxygen, DOC and nutrient concentrations against time. A correction was made for the composition of the reservoir water that replaced each sample.

e. Sediment properties

Total organic matter, organic carbon and nitrogen were determined on the freshly sieved sediment before the experiment started and on surface sediment from all microcosms after the experiment was completed. The organic matter content (OM) was determined as loss upon ignition at 500°C for 12 h. Particulate organic carbon (POC) and particulate organic nitrogen (PON) were determined with a Perkin Elmer 2400 CHN elemental analyser.

At the end of the experiment, on day 39, the cores were sliced. Porosity was calculated from water loss after drying at 110°C to constant weight (no salt correction). Bacterial measurements were made on 2 g fresh sediment samples collected from 0.5 cm, 1.5 cm, 3 cm, 6 cm and 12 cm. The DNA intercalating dye (DAPI) and two Cy3-probes (EUB 338, eubacteria, and SRB, sulphate-reducing eubacteria) were used on sediment samples to determine the total numbers of bacteria stained with DAPI and the percentages of active eubacteria (% EUB/DAPI) and active sulphate-reducing eubacteria (% SRB/DAPI). The sediment samples were prepared according to Mermillod-Blondin *et al.* (2005). Photosynthetic pigments concentrations (Chlorophyll *a* and phaeophytin) were determined at the same depths as bacterial measurements, by using a fluorometer according to Riaux-Gobin and Klein's protocol (1993).

Total wet biomass and biovolume of the animals, and the burrowing depths, the burrow radii and the thicknesses of the oxidized layers around burrows or animals were measured or estimated for each core.

Burrow radius calculations for each species used the measured biovolume (BioV) and the formula: $r = \sqrt{BioV \div [(\pi \times L)]}$, where L is the measured animal length. In the case of the mollusks, the allometric relationships of Zwarts and Blomert (1992) were assumed, where $W_{Ma} = 0.38L_{Ma} - 0.5$ and $W_{Mb} = 0.5L_{Mb} - 0.94$, and W_{Ma}, W_{Mb}, L_{Ma}, L_{Mb} are the *M. arenaria* and *M. balthica* estimated widths and measured shell lengths respectively. *Nereis* burrows were cylindrical and the assumed radii corresponded to the burrow openings measured at the sediment surface.

The average radius of each species (r) was then used to establish the minimum total species burrow volumes (ΣBurV) in the microcosms. Burrows were considered cylindrical, giving: $\Sigma BurV = n \times \pi \times [(r^2 \times L) + (r_{siphon}{}^2 \times h_{siphon})]$, where n is the total individual number of individuals in each core, r_{siphon} is the siphon radius, and h_{siphon} is the siphon length ($h_{siphon} = (h\text{-}L)$ with h the minimum burrowing depth measured for each species).

The mean thickness of the oxidized layer (OxT) in each microcosm was used to calculate the minimal oxic volume (OxV), which was considered also to be cylindrical, using the formula: $OxV = n \times \pi \times [(r+OxT)^2 \times L) + (r_{siphon} + OxT)^2 \times h_{siphon})] - \Sigma BurV$.

f. Statistical analysis

i. Benthic fluxes. One-way analysis of variance was applied to fluxes of oxygen, inorganic nutrients, and DOC measured on day 12, before introducing the animals, to verify low variability among the groups of microcosms assigned to individual treatments. Ammonium fluxes were then plotted together with oxygen, phosphate and nitrate fluxes at each

measurement date to resolve the general stoichiometric relationships and flux magnitudes characterizing the experimental systems with time. Oxygen fluxes into sediment were also plotted against nitrate and phosphate fluxes (flux sign convention: negative into sediment, positive out of sediment). Linear regression models II (major axis; Legendre and Legendre, 1998) were used for the flux correlations, and the slope calculations allowed determination of the apparent stoichiometric N/P and O/N ratios. The oxygen and nutrient fluxes on the final date of sampling were plotted versus the total oxic volume (cm^3) measured in all cores at the end of the experiment, and a linear regression model II was used to evaluate correlations.

The effects of single and assembled species treatments on net fluxes were then specifically compared using one-way repeated analyses of variance on flux measurements with time as the repeated factor and treatment as the main factor by using the Fisher-Snedecor test (Zar, 1998). An observed random variable (F_{obs}), with k ($p - 1$) and r ($n - k$) freedom degrees, where p and k are the sample and measurement number respectively, is compared with the theoretical F_{theor} at a 0.05 risk threshold. If F_{obs} (k,r) $> F_{theor}$, the two variances are different at the considered threshold (0.05). The homogeneity of variances among treatments was verified with the Bartlett test (Zar, 1998).

Principal component analysis (PCA), using Primer version 5 software (@copyright 2001 PRIMER-E Ltd), with the fluxes as variables and the functional treatments as observations, was used to visualize how species treatments were partitioned by the complete set of solute fluxes.

The effect of interactions on fluxes was estimated by subtracting from the observed fluxes model values one might have predicted without interactions. The predicted model values were calculated using a linear combination model by adding the flux values determined in single species treatments weighted by relative biovolume. For example, in a triplicate treatment that combines *M. balthica* and *M. arenaria,* the predicted flux is [Mb $(12\ mL)_{n=3}$ + Ma $(12\ mL)_{n=3}$]/2, whereas in a treatment combining the two bivalves and *N. virens,* the predicted flux would be: [Mb $(12\ mL)_{n=3}$ + Ma $(12\ mL)_{n=3}$ + Nv $(12\ mL)_{n=3}$]/3. In each case, terms of the form: Mb $(12\ mL)_{n=3}$, refer to the net flux observed in the presence of the single species Mb at a total biovolume of 12 mL.

ii. Sediment properties. The organic matter concentration and the C/N ratio were compared among treatments with one-way analyses of variance, using treatment as the main factor. Tukey *post hoc* tests were used to examine differences among treatments and dates.

For the photosynthetic pigments and the microbial population parameters, the treatment effect was tested with a one-way repeated measure ANOVA with treatment as main effect and depth as repeated factor because a measure at one depth is dependent on measures at adjacent depths, using the Snedecor-Fisher test. If significance was detected among treatments, Tukey post hoc tests were performed to determine which treatments differed. When homoscedasticity was not observed, microbial variables expressed as percentages were arcsine transformed (Zar, 1998).

Linear regression models I and II (major axis; Legendre and Legendre, 1998) were used to examine possible correlations between the microbial characteristics and the oxic volumes measured in the cores at each depth at the end of the experiment. Because bacterial abundances were made only at six depths, values in unmeasured intervals were interpolated between adjacent measurements and used for comparison with oxic volumes in the same intervals.

Differences between observed and predicted values, when the species are assembled, were tested with a one-way repeated analysis of variance using time as the repeated factor and treatment as the main factor. For microbial variables, observed and predicted values were compared using a two-way ANOVA with observed-predicted and depth as main effects.

3. Results

a. Visual observations and burrow structure

Individual *N. virens* occasionally left their burrows during the dark periods in the single species treatments, and we observed mucus-wrapped sediment on the sediment surface. *M. balthica* fed on surface deposits throughout the experiment, extending their siphons regularly and depositing numerous faecal pellets on the sediment surface. In contrast, *M. arenaria* never extended their siphons above the sediment surface; they merely stretched and withdrew the siphons within the sediment column at irregular intervals. The siphon openings of *M. arenaria* were sometimes covered by sediment, making them invisible. When several species were combined, the observations for each were similar.

The burrow openings in each core were measured and counted during the experiment (Table 2). The number of openings corresponded to the number of individuals in the cores (e.g. 12 openings in the cores containing 12 *Nereis*). Visual observations did not allow accurate description of each burrow in the sedimentary column, but some burrows appeared to be L or I shaped, rather than U or Y shaped. The diameters of the *Nereis* openings differed among treatments (Table 2). Larger openings were observed in the cores containing *N. virens* alone and in the (Mb + Nv) treatments, whereas smaller openings were observed in the (Ma + Nv) treatments. The *Nereis* burrow openings in the (Mb + Ma + Nv) treatments were about 4 mm in diameter.

When the cores were opened at the end of the experiment, the oxidized zones, defined here by the presence of discernable Fe-oxides, were revealed by the brown color of the sediment. The total thickness of the oxidized (and suboxic) zones in cores and around animals are presented in Table 2, assuming the average burrowing depth observed for each species and a steady state irrigated burrow distribution. Each animal was considered as a cylinder whose radius was calculated from animal biovolume as noted previously. *Nereis* burrows have a cylindrical shape with assumed radii corresponding to the burrow opening diameters. *Mya* and *Macoma* burrow radii were respectively calculated as 0.46 and 0.33 cm based on shell dimensions rather than siphon diameter. For comparison, Zwarts

Table 2. Synthesis of visual observations at the end of the experiment. Total number of burrow openings were counted and diameter of openings (cm) were measured. Minimum burrowing depth (h) (cm) for each species and averaged oxidized zone thickness (OxT) (cm) that we observed around animals are indicated. The minimum expected total volume for each species burrow (ΣburV) (cm^3) and the minimum expected total oxidized volume (OxV) (cm^3) in the cores were calculated from these last data, including the radius data obtained from biovolume (BioV) of each species. Mb; *M. balthica,* Ma: *M. arenaria;* Nv: *N. virens.*

Treatments	Burrow opening number	Burrow opening diameter (cm)			Minimum burrowing depth, h (cm)			Averaged oxidized zone thickness, OxT (cm)			Min. exp. tot. species burrow Vol. (ΣBurV) (cm^3)	Min. exp. tot. oxid. Zone, OxV (cm^3)
		Mb	Ma	Nv	Mb	Ma	Nv	Mb	Ma	Nv		
Control								0.5				39
Mb	24	0.1			2			0.2			12	61
Ma	6		0.7			6			0.5		18.9	79
Nv	12			0.5			12			0.2	28.3	103
Mb+Ma	12+3	0.1	0.7		2	6		0.2	0.5		15.5	70
Mb+Nv	12+6	0.1		0.6	2		12	0.2		0.4	26.4	141
Ma+Nv	3+6		0.7	0.2		6	8		0.5	0.4	11	95
Mb+Ma+Nv	8+2+4	0.1	0.7	0.4	2	6	12	0.2	0.5	0.4	16.3	108

and Blomert's allometric relationships (1992) gave *Mya* and *Macoma* respective radii as 0.55 and 0.33 cm based on the measured shell lengths and heights of individuals. These data allowed estimates of the total volume of burrows and the volume of oxidized sediment as a function of species and species mixtures (Table 2, Fig. 1).

The species-specific burrow volume/biovolume and oxic volume/biovolume ratios differed substantially in the order: *Nereis* > *Mya* > *Macoma* and were 2.33, 1.47, 1.07 (burrow volume/biovolume) and 5.26, 3.12, 1.97 (oxic volume/biovolume) respectively (e.g., Fig. 1a). As expected, a general linear relationship between total oxidized sediment volume and burrow volume extended across all microcosms, with a surficial sediment oxidized volume of ~39 cm^3 at 0 burrow volume (controls) (Fig. 1b). The species-specific ratios were used together with individual biovolumes to predict the total burrow volume and oxic volumes expected in species mixtures based on linear addition. Comparison of observed and model predicted total burrow and oxic volumes demonstrated good agreement for the Mb + Ma mixture but modest or substantial departures otherwise (Fig. 1c,d). The observed oxic volume was greater than predicted for all cases where *Nereis* was present and was particularly enhanced in the Mb + Nv mixture.

At the end of the experiment, one individual of *Macoma* was dead in a treatment containing *M. balthica* alone. One juvenile nereid was discovered in each of two control cores, in the (Mb + Nv) treatments, and in one core each of the other treatments with the exception of the (Nv +M a) treatments. No significant differences in biomass and biovolume were observed between the beginning and the end of the experiment (Table 1).

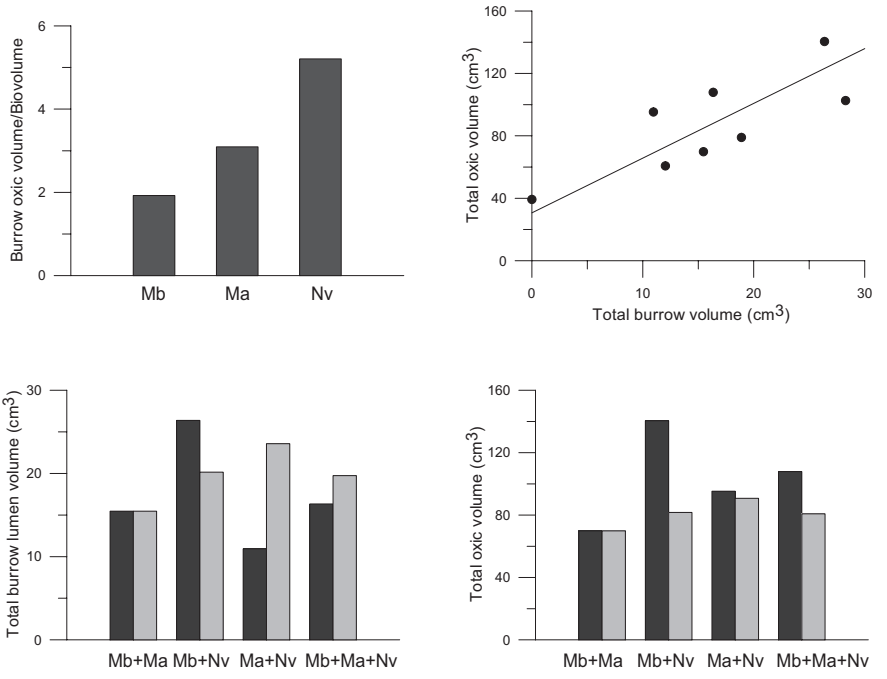

Figure 1. (a) Burrow oxic volume/biovolume ratios for single species treatment. *M. balthica* (Mb), *M. arenaria* (Ma), *N. virens* (Nv). (b) Correlation between total oxic volume (cm^3) and total burrow volume (cm^3). The equation for the plotted line is $y = 3.51x + 30.65$, $r = 0.80$, $p<0.05$. (c) Total burrow lumen volume for combined species treatments, Mb+Ma, Mb+Nv, Ma+Nv, Mb+Ma+Nv. (d) Total oxic volume (cm^3) for combined species treatments, Mb+Ma, Mb+Nv, Ma+Nv, Mb+Ma+Nv. Black and grey bars are the observed and predited values, respectively.

b. Benthic fluxes

i. Flux magnitudes and stoichiometric ratios. Ranges of the solute concentrations in overlying water, at the first time series sample for the fluxes measurements (t_0), were 1.45 to 2 mg O_2 L^{-1}, 30 to 80 mg DOC L^{-1}, 93 to 153 μmol NH_4^+ L^{-1} (except on day 20, 2 to 22 μmol NH_4^+ L^{-1}), 6 to 13 μmol NO_3^- L^{-1}, 1 to 4 μmol PO_4^{3-} L^{-1}.

Fluxes of dissolved oxygen, nutrients, and DOC measured on day 12 immediately before introducing macrobenthos, were comparable in all 24 microcosms (Table 3). As the fluxes on days 28 and 36 did not vary significantly with time, they were averaged for these two last dates. Plots of ammonium fluxes versus oxygen and phosphate fluxes are presented in Figures 2a and 2b for the dates 12, 20 and 28–36 days. These showed a regular progression of increasing magnitude and changes in net stoichiometric balances with time. No significant linear regressions between fluxes were measured before the introduction of the organisms on day 12. Subsequently, both NH_4^+ and O_2 fluxes increased with time and were closely correlated at dates 20 and 28–36 (respective regression coefficients of -0.70 and -0.95 ($p < 0.05$)). The slopes of these regressions (O_2/N) were -1.08 and -0.5,

Table 3. The averaged O_2, DOC, PO_4^{3-}, NH_4^+ and NO_3^- fluxes between the 24 microcosms measured on day 12 immediately before introducing animals. The fluxes were indistinguishable in the 24 microcosms ($F_{obs} > F_{theor}$, $p > 0.05$).

Measured fluxes	Averaged values	Snedecor-Fisher test
O_2 (μmol $O_2 \cdot h^{-1} \cdot m^{-2}$)	-180 ± 12	$F_{(7,16)} = 1.02$, $p>0.45$
DOC (mg DOC $\cdot h^{-1} \cdot m^{-2}$)	7.2 ± 3.5	$F_{(7,16)} = 0.75$, $p>0.63$
PO_4^{3-} (μmol $PO_4^{3-} \cdot h^{-1} \cdot m^{-2}$)	6.77 ± 0.75	$F_{(7,16)} = 0.40$, $p>0.88$
NH_4^+ (μmol $NH_4^+ \cdot h^{-1} \cdot m^{-2}$)	65.3 ± 21.5	$F_{(7,14)} = 0.40$, $p>0.88$
NO_3^- (μmol $NO_3^- \cdot h^{-1} \cdot m^{-2}$)	17.1 ± 7.7	$F_{(7,15)} = 0.89$, $p>0.53$

respectively, showing that the net stoichiometric O_2/N ratio decreased with time (i.e., became relatively N rich). Significant linear regressions were also determined between ammonium and phosphate effluxes for the dates 20 ($r = 0.75$, $p < 0.05$) and 28–36 ($r = 0.76$, $p < 0.05$). N/P ratios tended to increase between the date 20 (N/P = 13) and the date 28–36 (N/P = 25). Ammonium and nitrate were negatively correlated (date 20: $y = 4.04x + 152.26$, $r_{NH4+/NO3-} = -0.50$; date 28–36: $y = 4.50x + 504.42$, $r_{NH4+/NO3-} = -0.81$, $p < 0.05$, graph not shown), ammonium effluxes increase when nitrate is consumed, and at the same time, nitrate consumption is positively correlated with oxygen uptake (date 20:

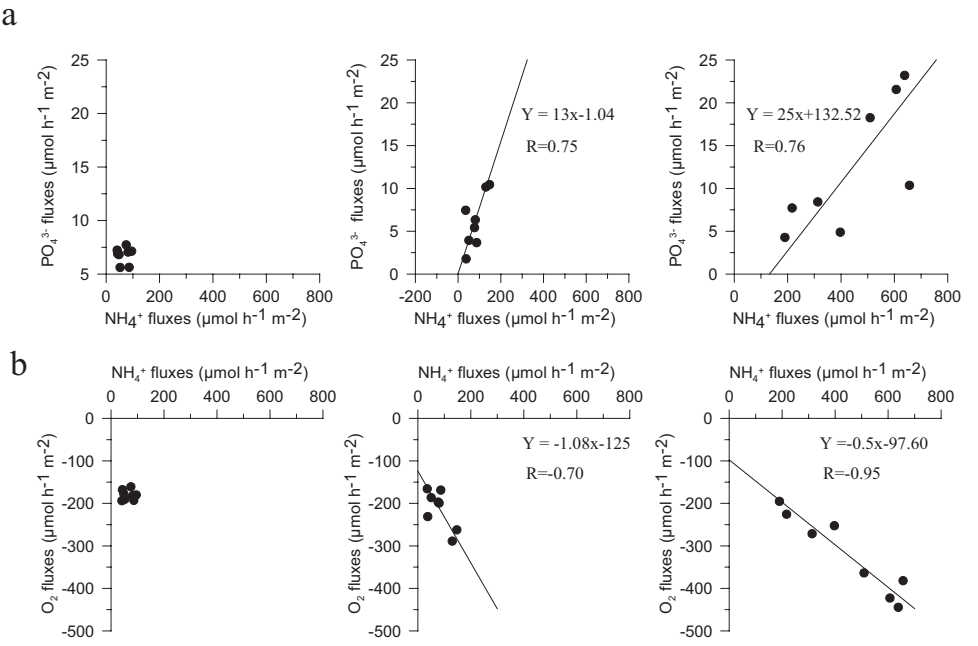

Figure 2. Correlations between (a) ammonium and phosphate fluxes and (b) between ammonium and oxygen fluxes at the three dates of the experiment (day 12, day 20 and day 28–36). The equations for the plotted lines are indicated on each graph.

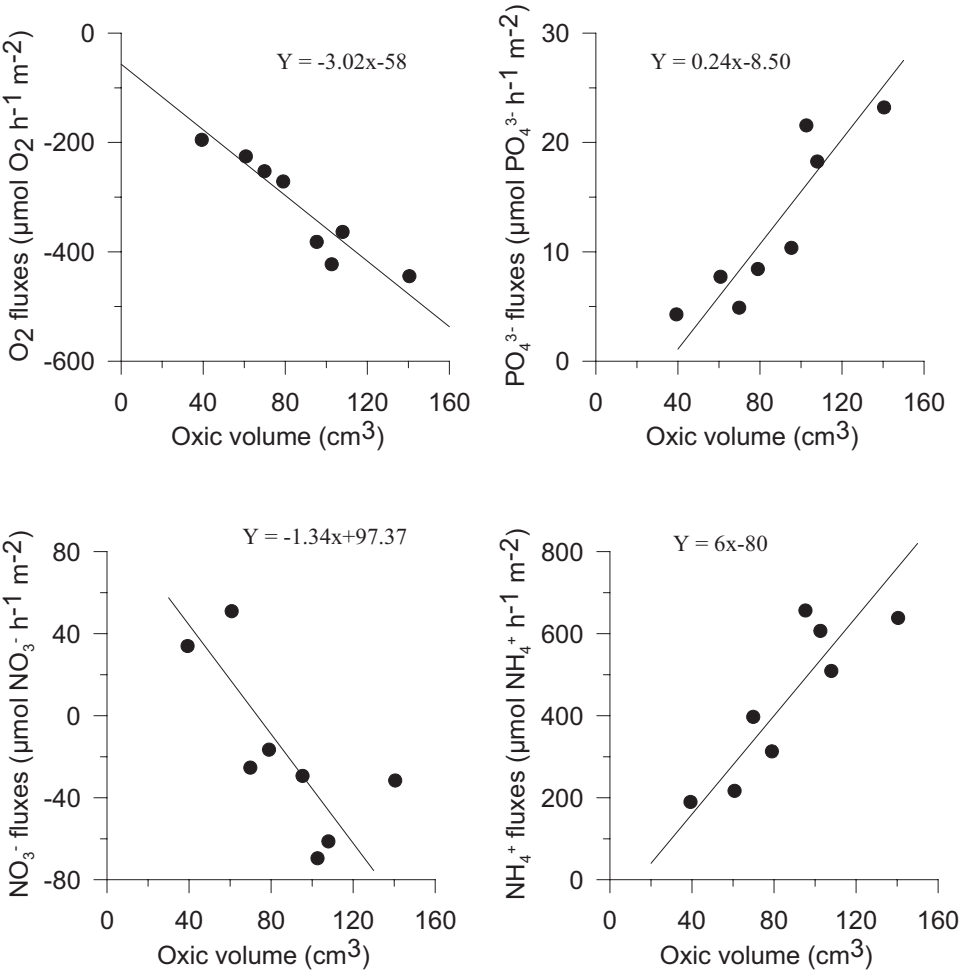

Figure 3. Correlations between oxygen and nutrient fluxes, and the oxic volumes measured around species. The equations for the plotted lines are indicated on each graph.

$y = 4.4x + 134.37$, $r_{O2/NO3-} = 0.44$; date 28–36: $y = 2.26x - 277.57$, $r_{O2/NO3-} = 0.80$, $p < 0.05$, graph not shown). In parallel, phosphate effluxes vary directly with oxygen uptake (date 20: $y = -14.38x + -124$, $r_{O2/PO43-} = -0.57$; date 28–36: $y = -12.6x$-164.32, $r_{O2/PO43-} = -0.91$, $p < 0.05$, graph not shown).

The oxygen and nutrient fluxes on days 28–36 are very well correlated with the sediment total oxic volumes, which are dominated by burrow wall contributions (Table 2) ($r_{O2/Ox.Vol.} = -0.93$, $r_{PO43-/Ox.Vol.} = 0.90$, $r_{NO3-/Ox.Vol.} = -0.73$, $r_{NH4+/Ox.Vol.} = 0.87$, $p <$ 0.05) (Fig. 3). Correlations were also measured between EUB, SRB and DAPI stained bacterial abundances and the total oxic volume (Fig. 4, Table 4).

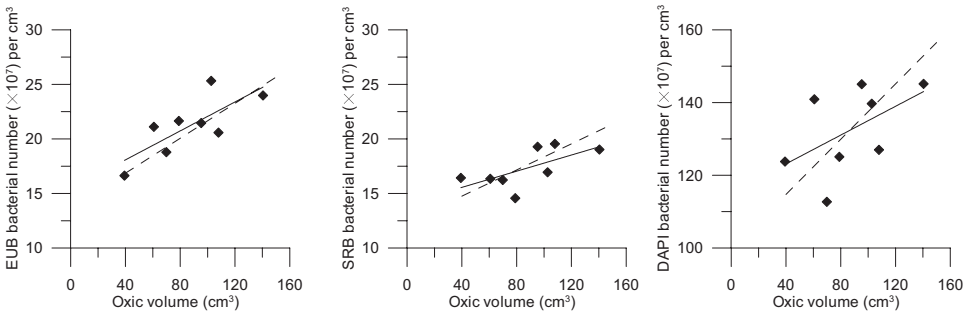

Figure 4. Correlations between the EUB, SRB and DAPI bacterial abundances (balanced for the whole sedimentary column in each microcosm) and the oxic volume measured around species. The filled and dotted lines respectively represent model I and II linear regressions whose the respective equations are in Table 4.

ii. Effects of species treatment on fluxes. The fluxes measured in each treatment are presented in Figure 5 as averages of the fluxes measured on days 28 and 36 (positive fluxes are out of the sediment, negative fluxes are in) in association with the total oxic volumes inside the cores measured on day 39. All treatments increased the oxygen flux over the control, but only *N. virens,* alone or combinations including *Nereis,* enhanced the flux at the statistical significance level ($p < 0.05$). The fluxes of DOC were slightly lower in microcosms with animals than in the controls with the exception of Mb+Ma. However, the only significant difference was with *N. virens* alone. The ammonium flux was higher in the presence of animals than in the control and highest in the four treatments containing *N. virens.* The nitrate flux was negative except in the control and in the single species treatment containing *M. balthica.* The highest phosphate fluxes were observed in the treatments containing *Nereis virens* alone, in combination with *M. balthica,* and combina-

Table 4. Results of statistical tests made on correlation coefficient (Fisher-Snedecor test) and on slope of each linear regression (Student t-test) in Figure 4. * indicates significance of the statistical tests at $p = 0.02$.

	Model I			Model II		
		Fisher-Snedecor $F_{(0.95;\,1;\,6)} = 5.99$	t-test $T_{(0.80,\,6)} = 0.9$		Fisher-Snedecor $F_{(0.95;\,1;\,6)} = 5.99$	t-test $T_{(0.80,\,6)} = 0.9$
EUB/OxV	Y=0.08x+15.42 R=0.76	*F =9.86	*T=1.55	Y=0.08x+13.66 R=0.76	*F =11.08	*T=1.80
SRB/OxV	Y=0.04x+14.07 R=0.67	*F =6.18	*T=1.23	Y=0.06x+12.35 R=0.65	*F =8.97	*T=1.63
DAPI/OxV	Y=0.2x+115 R=0.52	*F =145	T=0.83	Y=0.38x+99.52 R=0.52	*F =110*	T=1.40

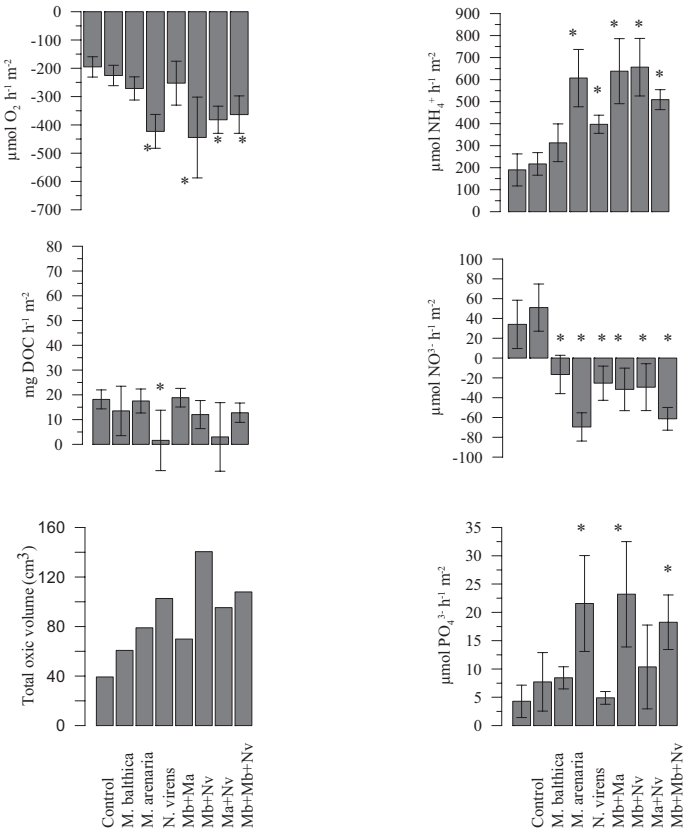

Figure 5. Fluxes of oxygen (O_2), dissolved organic carbon (DOC), ammonium (NH_4^+), nitrate (NO_3^-) and phosphate (PO_4^{3-}), across the sediment-water interface for the eight treatments (control, *M. balthica* (Mb), *M. arenaria* (Ma), *N. virens* (Nv), Mb+Ma, Mb+Nv, Ma+Nv, Mb+Ma+Nv) averaged on days 28 and 36 and the corresponding total oxic volumes measured int the same eight treatments. Fluxes are given as mean of ± SD of 3 microcosms. * indicates treatments that differed significantly from the control ($p < 0.05$) after performing Anova for each flux ($F_{(7,15)}$ (DOC) = 5.95; $F_{(7,16)}$ (O_2) = 21.51; $F_{(7,16)}$ (NH_4^+) = 23.05; $F_{(7,13)}$ (NO_3^-) = 20.70; $F_{(7,15)}$ (PO_4^{3-}) = 11.60) and HSD Tukey post hoc tests ($p < 0.05$).

tion with both bivalves. The effects of these three treatments were significantly greater than in the treatment combining *Nereis* with *M. arenaria.*

The principal components analysis (PCA) indicates that the first and second PCA axes explain 62% (eigenvalue of 3.09) and 16% (eigenvalue of 0.80) of the total variance. Oxygen and nitrate influxes, and DOC effluxes are positively correlated on the first PCA axis (Fig. 6a). Ammonium and phosphate effluxes are positively correlated on the opposite side of the first PCA axis. The samples are clustered into two groups (Fig. 6b): one group comprising treatments with *N. virens* alone or in combination with the bivalves, and a second group comprising the treatments without *N. virens.*

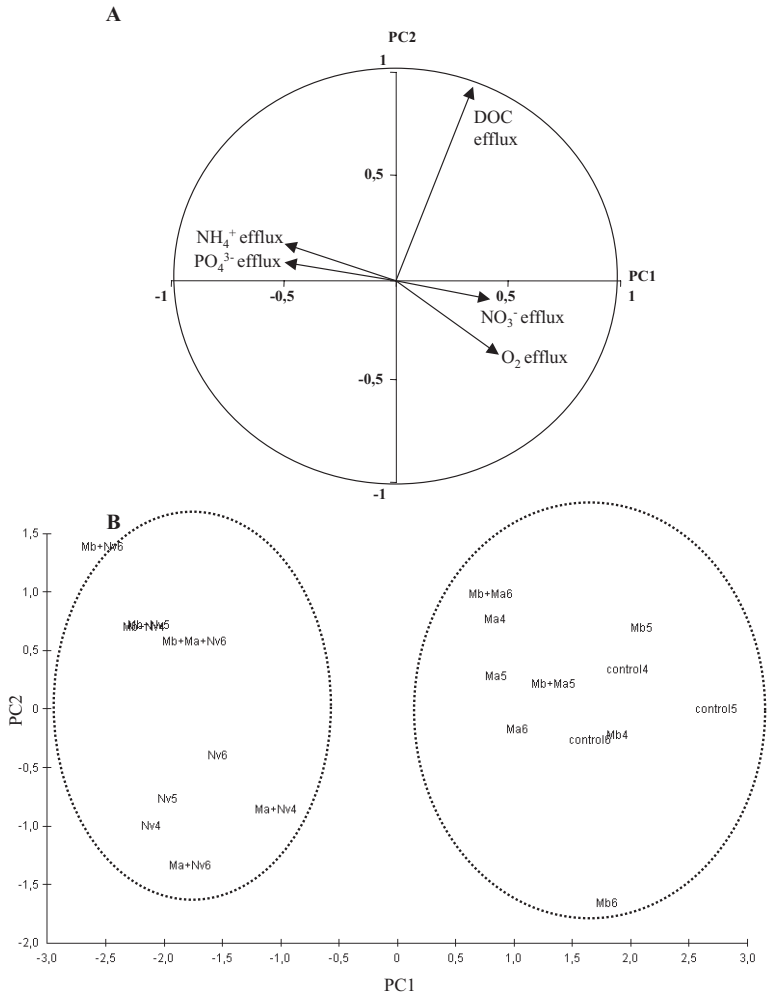

Figure 6. (A) The correlation circle for the Principal Component Analysis with O_2, NO_3^-, PO_4^{3-}, NH_4^+, and DOC fluxes as explaining variables on the first axis. (B) Position of the species assemblages (treatments) on the two first PCA axes. The numbers 4, 5, 6 are the replicate numbers for each treatment used by the Primer software.

iii. Effects of species interactions. Figure 7 shows the differences between observed and linear addition model fluxes in microcosms with two or three species combined. Most of the observed fluxes differ significantly from the fluxes predicted from a linear addition model. The discrepancies between observed versus predicted fluxes largely track the magnitudes of discrepancies between observed and predicted oxic sediment volume, with the presence or absence of Nereis being particularly critical (Figs. 1, 7). Oxygen uptakes measured are higher than predicted values by a fraction of 0.4× and 0.2× when N. virens

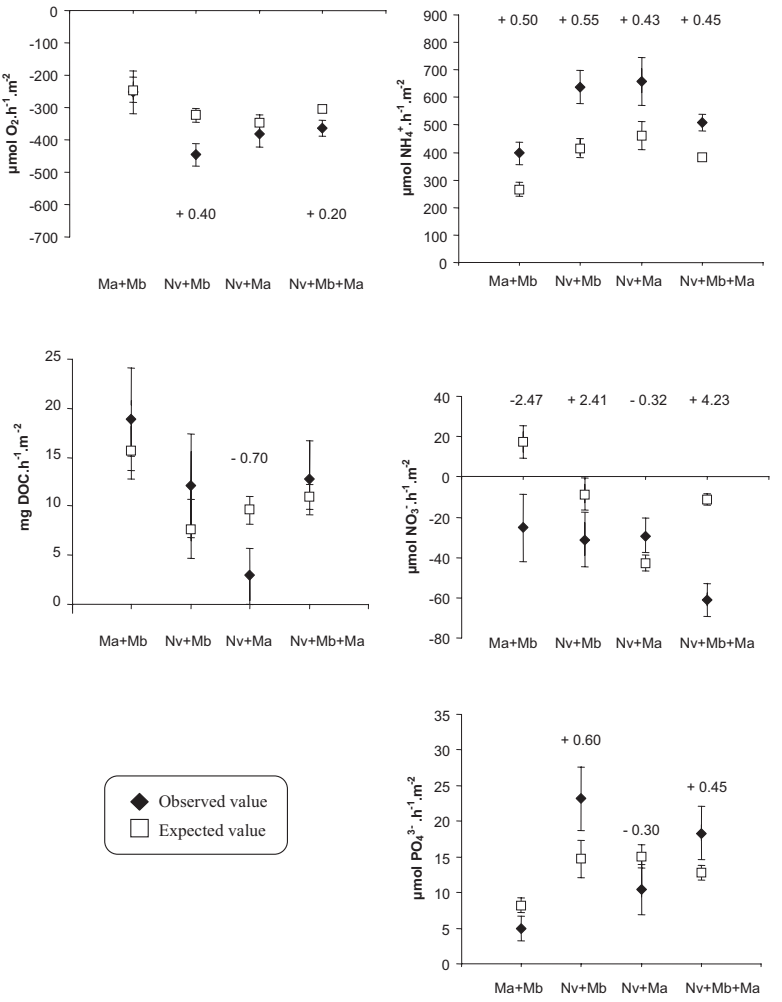

Figure 7. Comparisons between measured and predicted $O_{2,\,DOC}$, PO_4^{3-}, NH_4^{+}, NO_3^{-} fluxes across the sediment-water interface for the four species combined treatments (Mb + Ma, Mb + Nv, Ma + Nv, Mb + Ma + Nv) averaged from day 28 to day 36. Rates are given as mean of ± SD of 3 microcosms. The factor by those the observed values differ significantly from predicted values (*$p < 0.05$) is indicated for each case.

(Nv) is combined with M. balthica (Mb) ($F_{(1,22)} = 45.42$; $p < 0.0001$), and with both bivalves ($F_{(1,22)} = 23.71$; $p < 0.0001$) respectively. Oxygen uptake observed with the combination of *M. balthica* and *M. arenaria* (Ma) follows the linear addition model, and the combination of *N. virens* with *M. arenaria* nearly so. DOC consumption is modified by negative interactions between Nv and Ma ($F_{(1,22)}=19.60$; $p < 0.002$), compared to the predicted value by $-0.7\times$. Among nutrient fluxes, ammonium effluxes measured were

Table 5. Loss on ignition (LOI), particulate organic carbon (POC) and nitrogen (PON), molecular C/N ratio in freshly sieved sediment at the beginning of the experiment and in the surface layer (0–0.5 cm) of the microcosms (control, *M. balthica* (Mb), *M. arenaria* (Ma), *N. virens* (Nv), Mb + Ma, Mb + Nv, Ma + Nv, Mb + Ma + Nv) at the end of the experiment (means ± SD, n = 3).

Treatment	LOI (%)	POC (μmol g^{-1} DW)	PON (μmol g^{-1} DW)	C/N ratio
Beginning of the experiment				
	1.88 ± 0.16	182 ± 17	19.9 ± 2.5	9.2 ± 1.6
End of the experiment				
Control	1.91 ± 0.30	325 ± 125	29.9 ± 5.9	10.6 ± 2.1
M. balthica	1.86 ± 0.28	237 ± 59	14.5 ± 8.0	20.8 ± 12.1
M. arenaria	1.80 ± 0.14	255 ± 64	20.8 ± 7.8	12.9 ± 3.3
N. virens	1.99 ± 0.05	295 ± 72	31.0 ± 7.6	9.9 ± 3.1
Mb+Ma	2.09 ± 0.16	263 ± 83	19.5 ± 12.4	17.4 ± 11.4
Mb+Nv	1.76 ± 0.15	225 ± 20	9.4 ± 1.1	24.1 ± 5.1
Ma+Nv	1.85 ± 0.15	258 ± 19	17.6 ± 1.3	14.7 ± 1.6
Mb+Ma+Nv	1.90 ± 0.18	215 ± 8	15.4 ± 4.4	14.7 ± 4.3

increased compared with the predicted values for all the species combinations: the combination of Nv with Mb increased the predicted value by the greatest percentage of 0.55× ($F_{(1,22)} = 50.82$; $p < 0.0001$), followed by the combination of Mb and Ma ($F_{(1,22)} =$ 34,07; $p <$ 0,0001), Nv and Ma ($F_{(1,22)} = 18.89$; $p < 0.001$), and the three species together ($F_{(1,22)} = 64.99$; $p < 0.0001$). Likewise, all species combinations led to interactive effects on nitrate fluxes. The highest positive interactive effects were measured between Nv and Mb ($F_{(1,22)} = 10.35$; $p < 0.009$) and between all three species ($F_{(1,22)} = 147.9$; $p <$ 0.0001). The combination between the two bivalves ($F_{(1,22)} = 26.43$; $p < 0.001$), and between Nv and Ma led to high negative interactions with nitrate fluxes ($F_{(1,22)} = 10.94$; $p < 0.009$). Phosphate fluxes measured were significantly modified with predicted fluxes from a linear addition model, only when Nv was combined with the bivalves. The combination between Nv and Mb ($F_{(1,22)} = 14.02$; $p < 0.04$), and between Nv, Mb and Ma ($F_{(1,22)} = 8.32$; $p < 0.008$) led to positive interactive effects, whereas the combination of Nv with Ma led to modest negative interactive effects on phosphate fluxes ($F_{(1,22)} = 7.48$; $p < 0.023$) since the observed mean value is lower than the predicted value of phosphate fluxes by a percentage of −0.32×.

c. Sediment particle properties

i. Chemical characteristics of the sediment. In situ porosity at the sediment collection site averaged 0.65. The porosities in microcosm cores averaged 0.6 in the surface 0–0.5 cm layer, 0.5 in the 0.5–12 cm layer, and 0.6 below 12 cm. The measurements of sedimentary organic matter, POC, PON and the C/N ratio at the beginning of the experiment and in the top layer of the sediment (0–0.5 cm) at the end of the experiment are given in Table 5. In

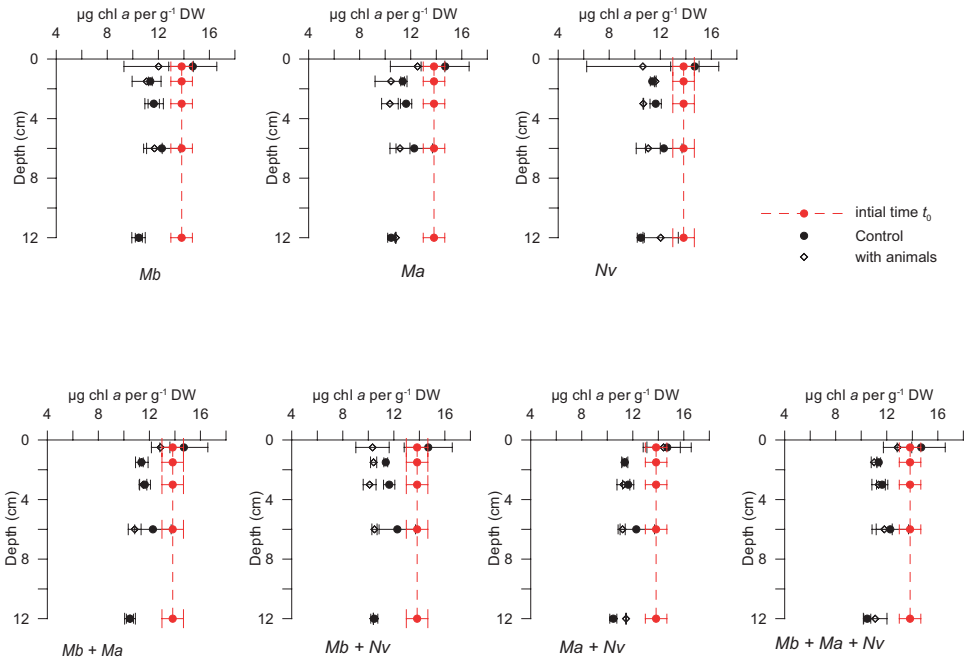

Figure 8. Chlorophyll *a* concentrations (µg chl *a* g^{-1} DW) over depth (cm) in the different treatments at the initial time (t_0) and at the final time.

the control microcosms, these variables tended to increase during the experiment, but the increases were not statistically significant. POC and PON parameters were lower in the inhabited treatments compared to the final control sediments. C/N ratios increased in all sediments with macrofauna. Only PON decreases are significant in the macrofauna relative to final control microcosms (ANOVA, $F_{(7,15)} = 2{,}82$; $p < 0.04$), specifically for Mb, Mb + Nv and Mb + Ma + Nv treatments (LSD post hoc tests, $p < 0.05$).

The photosynthetic pigments concentrations were 13.82 ± 1.04 µg g^{-1} DW Chl *a* and 4.14 ± 0.38 µg g^{-1} DW phaeophytin in the tank sediments at the beginning of the experiment, leading to Chl *a*/Phaeophytin ratios averaging 3.35 ± 0.10. These initial values were constant with depth. The final Chl-*a* profiles were characterized by surface values (0–1.5 cm) that were either the same or very slightly increased from the initial value (Fig. 8). Below the surface 1.5 cm, Chl-*a* concentrations were constant with depth but always lower than the starting value, ranging from ~10–11 µg g^{-1} DW. Statistical analyses showed a significant treatment effect ($F_{(7,68)} = 3{,}21$; $p < 0.005$), with Chl *a* concentrations below 1.5 cm lowest in the Mb + Nv treatment ($p < 0.05$). Otherwise, Chl-*a* concentrations tended to be lower in the inhabited sediments relative to control for all sediment layers, except in the deepest layer (>12 cm) occupied by either *Nereis virens* alone or in combination with the other species. In contrast, phaeophytin increased slightly with time in all depth intervals in inhabited sediments (~5–6 µg Ppt-a g^{-1} DW) and more

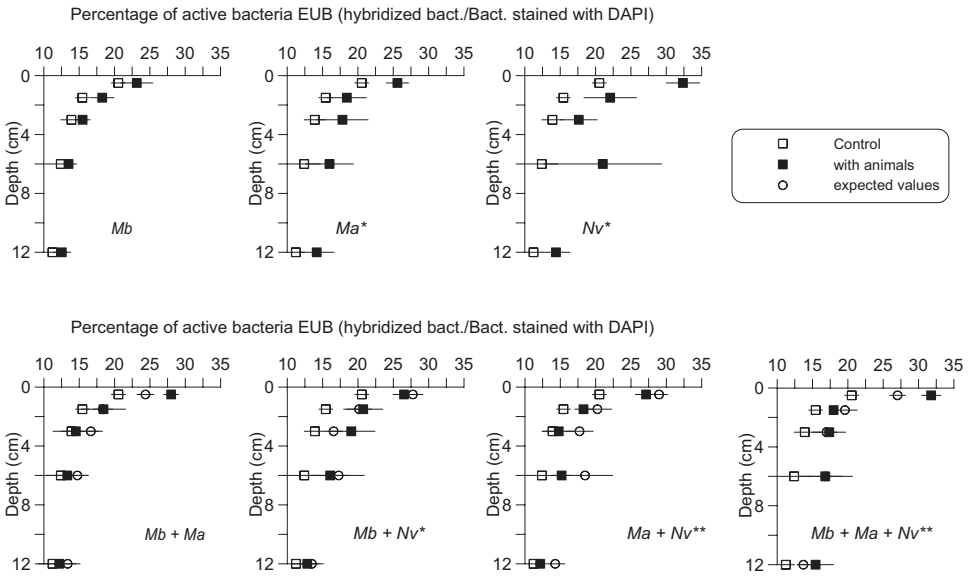

Figure 9. Vertical profiles of the percentage of active eubacteria for the eight treatments (mean ± SD n=3) that differ significantly with depth ($F_{(4,8)} = 91.55$, $p < 0.0001$). Control profiles are indicated. * indicates treatments that differed significantly from the control ($F_{(7,8)} = 9.05$, $p < 0.05$; HSD Tukey: $p < 0.001$). Profiles resulting from the predicted values were added for comparison with observed values. ** indicates significant difference from predicted values ($p < 0.05$).

so in the controls (6–15 μg Ppt-a g^{-1} DW) with no statistically significant depth dependence (data not shown). The final Chl *a*/Phaeophytin ratio averaged 1.8 in control cores and ~2–2.5 in inhabited cores.

ii. Microbial characteristics of the sediment. The total number of bacteria (bacteria stained with DAPI) decreased significantly with depth (data not shown), and bacterial abundances measured at 6 and 12 cm were lower than those observed at the surface. There was no statistically significant effect among treatments for the total number of bacteria, although a rough positive correlation between DAPI stained bacteria and oxic volume was evident with the regression model II (Fig. 4, Table 4). The percentage of the bacteria that are active (bacteria hybridized with EUB related to bacterial cells stained with DAPI) decreased significantly with depth (Fig. 9) and was significantly different among treatments. The presence of *M. arenaria* alone and *N. virens* in all the treatments increased the percentage of EUB compared to the control. As noted previously, EUB, SRB, and DAPI stained bacteria correlated directly with total oxic volume and thus total burrow volume (Figs. 1, 4, Table 4; DAPI model I regression not significant at $p = 0.02$ level). The percentage of active sulphate reducing bacteria SRB decreased with depth (Fig. 10) and was affected by the treatments, particularly in single species treatments and in the Nv + Mb treatments. In

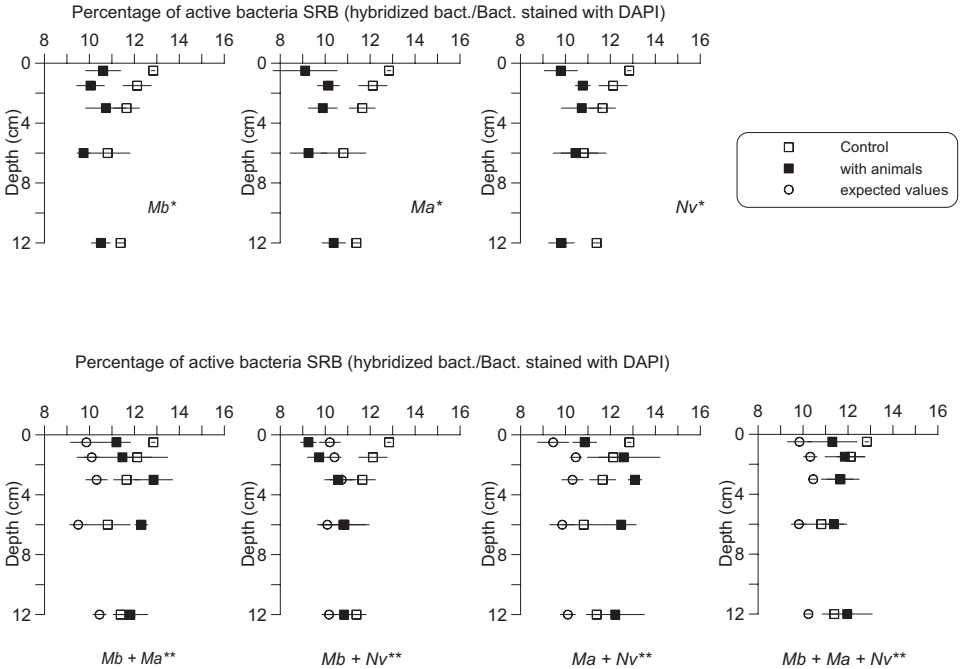

Figure 10. Vertical profiles of the percentage of active sulphate-reducing bacteria for the eight treatments (mean ± SD, n = 3) that differ significantly with depth ($F_{4,8} = 2.89$, $p < 0.03$). Control profiles are indicated on each graph. * indicates treatments that differed significantly from the control ($F_{(7,8)} = 19.89$, $p < 0.0001$; HSD Tukey: $p < 0.001$). Profiles resulting from the predicted values were added for comparison with observed values. ** indicates significant difference from predicted values ($p < 0.05$).

these treatments, animals reduced the percentage of SRB compared to the control, particularly in the uppermost sediment layers.

The microbial community showed several signs that it was affected by interactions among species beyond what was predicted by the linear addition model. Abundance of bacteria, percent active eubacteria, and percent active sulphate-reducing bacteria changed more than was predicted except in the Mb + Nv treatment (Figs. 9 and 10). The vertical profile of bacterial abundance was affected positively by interactions between the two molluscs (Mb + Ma) ($F_{(1,58)} = 10$; $p < 0.003$) and in the (Ma + Nv) treatment ($F_{(1,58)} = 7$; $p < 0.01$), whereas the abundances observed in the (Mb + Ma + Nv) treatment were lower than those predicted ($F_{(1,58)} = 10$; $p < 0.002$). Significant positive species interactions on the active EUB bacteria were only observed with the (Mb+Ma+Nv) treatment ($F_{(1,58)} = 10$; $p < 0.002$), whereas the (Ma + Nv) treatment led to negative interactions ($F_{(1,58)} = 13.09$; $p < 0.0001$). In all multispecies treatments, the percentages of sulfate reducing bacteria was higher than predicted ($F_{(1,58)\,(Mb+Ma)} = 116.84$; $F_{(1,58)\,(Nv+Ma)} = 138.33$; $F_{(1,58)\,(Mb+Ma+Nv)} = 7$; $p < 0.00001$).

4. Discussion

a. Experimental design and initial conditions: impact on the biogeochemical functioning of the experimental system

It is important to recognize that the experimental design played an important role in dictating the time dependent flux patterns and to some extent the macrofaunal impacts. In order to reduce inter-microcosm variability, the sediment used in the microcosms was first sieved and homogenized. The resulting sediment column lacked the strong vertical gradient in concentration and reactivity of organic matter typically found in steadily accreting deposits *in-situ.* Bacterial remineralization rates would therefore have been approximately constant over the depth of the microcosms rather than strongly decreasing with depth. The exception to this average pattern with depth would be enhanced remineralization within thin zones of oxic sediment near boundaries subject to efficient diffusive exchange of solutes (Aller and Aller, 1998; Sun *et al.,* 2002), and in surfacemost sediment subject to photosynthetic activity (Fig. 8). The experimental sediment also came from the first centimeter *in situ,* implying that it contained abundant fresh organic matter, an inference supported by the high Chl *a* concentrations in all microcosm depth intervals (around 14 and 10 μg Chl *a* g^{-1} DW at the beginning and the end of the experiment respectively). As a consequence, high rates of anaerobic remineralization were sustained at depth in tanks, resulting in progressive increases in anaerobic metabolite fluxes as pore water concentrations built-up, and a corresponding increase in O_2 uptake along sediment-water interfaces as total reoxidation of diffusing metabolites increased with time.

The lowered Chl-*a*/Ppt-*a* ratios at the end (~1.80 controls; 2–2.5 inhabited) compared to the beginning (3.35) of the experiment reflect a combination of Chl-*a* degradation and phaeophytin net production or stability. Dominant anoxic conditions may explain the slightly increased or relatively stable phaeophytin concentrations at depth, since it has been observed that Ppt, which derives from Chl-*a* degradation, degrades more slowly than Chl-*a* and remains stable under anoxic conditions (Sun *et al.,* 1993). The decrease in the Chl-*a*/Ppt ratio with time and the approximately constant Chl-*a*/Ppt ratio with depth below the surfacemost layer at any given time supports the inferences both of dominant anaerobic degradation pathways and of relatively constant rates of remineralization below the surface layer in all cases; whereas the lower average Chl-*a* at depth in inhabited relative to control cores implies comparatively enhanced degradation in the former.

The high and dominant rates of anaerobic metabolism at depth, and the unsteady ingrowth of pore water metabolites, are also reflected in the progressive change in net flux stoichiometries: decreasing O_2/NH_4^+ fluxes ratios with time (~1.1–0.5) (Fig. 2) and lack of any correspondence to steady–state Redfield average plankton compositions (~6.6). Under such conditions, the relative effect of deep burrows on fluxes such as O_2, NH_4^+, NO_3^-, or HPO_4^{2-} should have been accentuated compared to commonly encountered *in-situ* conditions and interpretations must be appropriately tempered. The experimental setup is a good analogue, however, to the responses and interactions expected *in situ*

following rapid deposition of redistributed surface sediment (e.g., a storm) and its recolonization by adult benthos (Graf *et al.,* 1982; Miron and Desrosiers, 1990).

b. Role of burrow structure, volume, and irrigation

Each species generated a different burrow volume relative to biovolume and oxidized the surrounding sediment during burrow irrigation. *N. virens* clearly formed and irrigated a greater volume of burrow lumen relative to its biovolume than did the bivalves (Fig. 1a), and *N. virens* is the dominant species in controlling flux patterns (Fig. 6). Because the penetration of O_2 around burrows depends on consumption rates in surrounding sediment, and because those rates were relatively constant volumetrically in the microcosm sediment, burrow volumes and oxidized sediment volume were closely correlated across all species and species mixtures regardless of burrowing depth (Fig. 1b). The biogenic formation of oxic sediment volume, which requires and indicates active irrigation, directly reflects the generation of actively inhabited burrow structures which provide three-dimensional conduits for solute exchange between sediment and overlying water. Thus, the magnitudes of the net fluxes of solutes produced or consumed during remineralization within the microcosm sediment directly track the biogenically and physically controlled oxic sediment volume (Fig. 3). As burrow construction becomes more complex with time (Michaud *et al.,* 2005), irrigation controlled diffusive fluxes from anoxic regions increase proportionately, producing progressively higher N/P ratios and lower O_2/N ratios. The extent of the burrow wall oxidized zones is also critically important because of the reoxidation of anaerobic metabolites which determines nitrification–denitrification balances, the oxidation of DOC released in surrounding anoxic zones, and the formation of Fe-oxides along burrow walls which differentially scavenge reactive solutes such as HPO_4^{2-} (resulting in high N/P flux ratios).

The enhanced exchange of solutes and the formation of oxidized microenvironments apparently increases both aerobic and coupled aerobic–anaerobic metabolism, stimulating overall bacterial activity, as indicated by DAPI, EUB and SRB assays of active bacterial abundances (Fig. 4). The increased volume of oxidized sediment in the inhabited cores increases the percentage of total bacteria that are actively aerobic (EUB) (Fig. 9) and decreases the percentage of bacteria that are sulfate reducers (SRB, Fig. 10) compared to the control sediments, however, the absolute numbers are increased in both cases (Fig. 4). The coupling and interaction between oxic volume and bacterial activity is complex. For example, increased oxic volume and metabolite exchange clearly allow increased EUB, but any increased bacterial activity also tends to decrease oxic volume. Increased oxic volume likewise acts as a sink for anaerobic metabolites (e.g. H_2S) produced in nearby anoxic regions, stimulating SRB adjacent to the oxic zone and promoting a decrease in oxic volume. Thus the relationships between these properties represent dynamic balances, and need not be exclusively dependent and independent. In recognition of these potential interactions, both model I and II regressions are depicted in Figure 4. Microbial (algal) and

meiofaunal biomass may explain the slight, but not significant, LOI and POC increases with time within the surface layer (0–5 cm) of microcosms.

c. Effects and mechanisms of species interactions

With the possible exception of DOC fluxes, the simple linear addition model based on biovolume did not accurately predict the effects of species mixtures on oxic (irrigated) burrow volume, net fluxes, or microbial properties in ~70% of the possible cases (Figs. 1, 7, 9, 10). A range of factors, including interactions among different feeding strategies, partitioning of food, increase in activity due to interferences, and the three-dimensional spatial organization of the community, may act alone or in combination to affect the net functioning (nutrient regeneration) of the ecosystem. Since our experiment was not designed to provide information on feeding strategies and food partitioning, we will not address these further, rather our discussion will focus on space occupation and its effects on biogeochemistry and fluxes.

i. Spatial organization and burrowing behavior. The fact that the number of burrow openings for *N. virens* was identical to the number of individuals present suggests that each burrow had a single opening, i.e. that the burrows were L-shaped or I-shaped rather than U-shaped or Y-shaped. Visual observations confirmed that at least some burrows were L or I shaped. Miron *et al.* (1991) found that for relatively low animal densities, *Nereis* creates U-shaped burrows with a volume double the volume of L or I-shaped burrows. This shape contrasts with the L and Y-shaped tubes found at higher densities. They concluded that space partitioning, and the shape and length of the burrows are density dependent; at lower density the animals create greater and deeper burrows with more branches and openings. Our results suggest that the number of openings, the shape and length of *Nereis* burrows, and the occupation–irrigation behavior also depend on the other species that are present. For example, the diameter of the burrow opening and the length of the burrows were smaller when *N. virens* was combined with *M. arenaria* than when it was alone or when it was combined with *M. balthica,* yet the total volume of the space occupied by the organisms in the treatments were not different and the oxic burrow volume was slightly more than predicted (Fig. 1).

Because of life habit differences, the spatial distribution of biovolume varied significantly among the treatments. In the 12Mb + 6Nv combination, the 6 *N. virens* combined with the 12 near-surface dwelling *M. balthica* were likely to have had more space available in the deep layers than the 6 *N. virens* that were combined with the 3 *M. arenaria* in the 3Ma + 6Nv combination. Each *N. virens* burrow in the (Nv) and (Nv + Mb) treatments (visual observations) had actually a diameter of 0.5 and 0.6 cm and a minimum length of 12 cm, giving an individual burrow volume of about 2.4 and 3.4 cm^3 respectively. The burrow volume was reduced by a factor of 9 to 13 when *N. virens* was associated with Ma, and by factor of 2 when *N. virens* was associated with the two bivalves (Table 2). The oxidized volume varied accordingly (Table 2). *M. arenaria* burrows deeper than *M. balthica*

and occupies space that could otherwise have been available to *N. virens.* The burrow volume/biovolume ratio of the Ma + Nv is less than predicted and shows possible spatial interference in the deeper layers between *M. arenaria* and *N. virens,* whereas the oxic volume is greater than predicted suggesting greater irrigation activities (Fig. 1c,d). Complementarity in space occupation, as in the (Mb + Nv) and (Mb + Ma + Nv) treatments, could reduce the intra-species competition of single species treatments whereas competition for space in the deeper sediment layer might reduce the extent of gallery formation.

Consequently, the size of a gallery network and the proportion of it that is irrigated have a strong influence on the rate of oxygen exchange across the water sediment interface, which would at least in part explain the positive relationship between the diameter and length of *N. virens* burrows and solute fluxes. Different spatial organizations could thus lead to different irrigation behavior and solute exchange rates, such as observed by Jorgensen *et al.* (2005) for Arctic fjord sediments and by Lewandowski *et al.* (2007) for lake sediments. Because oxygen uptake is proportional to oxidized volume, we conclude that the dependence of the spatial organization on interspecies interactions influences the exchange of oxygen and other solutes across the sediment-water interface, as well as the population of bacteria that inhabit burrow walls. Unfortunately our measures of behavior and activity (e.g., burrow volume and oxic volume) are indirect and ideally in future experiments they should be more directly quantified.

ii. Burrowing depth. Aside from burrow shape and spacing, burrowing depth also affects fluxes by tapping into deeper sediments that might otherwise not efficiently exchange with overlying water. These effects, as mentioned previously, are accentuated in the present experiment because the distribution of reactive organic substrates at depth, and thus anaerobic metabolite production, was enhanced by initial homogenization. We would expect reactions that respond to the coupling of oxygen and reduced solutes to be particularly affected, and indeed the greatest effects resulting from species interactions were on NO_3^- fluxes into sediment that were enhanced by -2.4, 2.4 and 4.2 relative to the predicted values with the (Mb + Ma), (Nv + Mb) and (Mb + Ma + Nv) treatments respectively. Denitrification, which in these circumstances must be largely supported by sedimentary nitrification rather than overlying water NO_3^- (Seitzinger *et al.,* 2006), was clearly dramatically enhanced by deep burrowing, as in addition to net NO_3^- fluxes from overlying water into sediment, all NO_3^- formed along oxic burrow walls was also consumed (Figs. 5, 7). Greater burrowing depths in species mixtures also enhanced ammonia (± 0.5), and phosphate (0.3 to 0.6) fluxes (Michaud *et al.,* 2006). Burrowing depths alone cannot explain the relatively weak mobilization of phosphate reflected in the low P/N stoichiometry of the net fluxes. We assume that oxidation and co-precipitation of phosphate with iron oxides in oxic sediment volume, for example, in the vicinity of the siphons of the bivalves, is primarily responsible for comparatively low net P fluxes (Sundby *et al.,* 1992).

Alteration of burrow aggregations and spacing therefore affects the total surface area of burrows, the diffusive coupling between solutes (e.g., nitrification–denitrification), microbial activity distributions, and, depending on reaction kinetics, the production rate of solutes. For example, Marinelli (1994) and Aller and Aller (1998) found respectively that (1) organisms could modify the barrier to solute diffusion offered by tube aggregations, and that (2) burrow spacing modified the scale of diffusion and altered the net production of metabolites such as NH_4^+. In addition, Gilbert *et al.* (2003) demonstrated a link between the rates of N remineralization and the balance between stimulation/inhibition of denitrification with sedimentary biogenic structures and the particular geometries of irrigated burrow distributions. They determined an optimal length between burrows that was appropriate for a maximal stimulation of denitrification. Thus, small changes in the thickness of adjacent oxic-anoxic zones around burrows are determining factors for sedimentary nitrification and denitrification. We did not make accurate measurements of the spatial arrangements of the burrows, or as mentioned previously, activity measures such as the production rate of burrows. Clearly spatial measurements need to be carried out in future studies of this kind with the use of resin casts (Gerino and Stora, 1991) or Cat-Scan, which has the advantage of being non destructive (see Michaud *et al.,* 2003; de Montety *et al.,* 2003; Dufour *et al.,* 2005, 2007; Rosenberg *et al.,* 2007).

5. Conclusions

The interactions between the dominant benthic species within the *Macoma balthica* community often, but not always, result in net fluxes of remineralized nutrients that cannot be accounted for in simple linear addition models based on single species effects normalized to biovolume. Most of the effects of single species and mixtures of species on solute fluxes can be directly linked to burrowing patterns, burrow volume, and in particular the volume of sediment oxidized by active irrigation. In the present experiments, net fluxes correlated directly with the volume of oxic sediment formed by benthic species. The interactions that determine burrow volume, burrow distribution, and extent of irrigation (oxidized sediment volume) thus determine the net fluxes. *Nereis virens,* which had the largest species specific burrow volume/biovolume ratio, was the single most important determinant of solute fluxes under the experimental conditions, however, species interactions such as competition for burrow space at depth, also affected net fluxes.

Therefore, the mechanistic basis of species interactions within sediments as reflected in biogenic structures need to be precisely quantified to develop and validate theoretical models of the role of biodiversity on ecosystem functions (i.e., benthic fluxes). Future work should take into account the dominant functional traits such as irrigation behavior and depth of burrowing but also the effects of species interactions on space occupation, including changes in the volume, distribution of burrows, and burrow production rates. More complex benthic communities with greater number of species and functional groups also need to be studied to investigate a wider range of functional interactions that may affect biogeochemical processes in deposits. Finally, interpretations of laboratory results

must take into account possible experimental artefacts, for example alteration of natural diagenetic reaction gradients, in order to assure the field-relevance of experimental studies.

Acknowledgments. We thank H. Holmes, J.-F. Lemieux and M. Dionne for permission to sample in the Parc national du Bic and Real Fournier for providing laboratory space in the Aquaculture Station at Pointe au Père. M. Laroche provided technical help, M. Gauthier, M. Dalva and D. Bérubé helped with the analysis of nutrients, DOC and CHN. Dr. S. Hulth provided helpful comments. The study was supported by grants from the Natural Sciences and Engineering Research Council of Canada to G. D. and B. S. and from the International Council for Canadian Studies to E. M. R. C. A. was supported by US NSF grant OCE0526410. This is Nereis Park contribution number 20. This manuscript was completed at Stony Brook University while E. M. was a research associate.

REFERENCES

Aller, R. C. 1982. The effects of macrobenthos on chemical properties of marine sediment and overlying water, *in* Animal Sediment Relations, P. L. McCall and M. J. S. Tevesz, eds., Plenum Press Press, NY, 53–102.

—— 2001. Transport and reactions in the bioirrigated zone, *in* The Benthic Boundary Layer: Transport Processes and Biogeochemistry, B. P. Boudreau and B. B. Jorgensen, eds., Oxford, University Press, Oxford, 269–301.

Aller R. C. and J. Y. Aller. 1998. The effect of biogenic irrigation intensity and solute exchange on diagenetic reaction rates in marine sediments. J Mar Res., *56,* 905–936.

Aminot, A. and M. Chaussepied. 1983. Manuel des analyses chimiques en milieu marin. Centre national pour l'exploitation des océans. Brest, 395 pp.

Cardinale, B. J., M. A. Palmer and S. L. Collins. 2002. Species diversity enhances ecosystem functioning through interspecific facilitation. Nature, *415,* 426–429.

de Montety, L., B. Long, G. Desrosiers, J.-F. Crémer, J. Locat and G. Stora. 2003. Utilisation de la scanographie pour l'étude des sédiments: influence des paramètres physiques, chimiques et biologiques sur la mesure des intensités tomographiques. Can. J. Earth Sci., *40,* 937–948.

Desrosiers G., J-C. Brêthes and B. Long. 1984. L'effet d'un glissement de terrain sur une communauté benthique médio-littorale du Nord du Golfe du St-Laurent. Ocean. Acta, *7,* 251–258.

Dufour, S. C., G. Desrosiers, B. Long, P. Lajeunesse, M. Gagnoud, J. Labrie, P. Archambault and G. Stora. 2005. A new method for three-dimensional visualisation and quantification of biogenic structures in aquatic sediments using axial tomodensitometry. Limnol. Ocean. Meth., *3,* 372–380.

—— 2007. Update: A new method for three-dimensional visualization and quantification of biogenic structures in aquatic sediments using axial tomodensitometry. Limnol. Ocean. Meth., *5,* 372–380.

Emmerson, M. C. and D. G. Raffaelli. 2000. Detecting the effects of diversity on measures of ecosystem function: esperimental design, null models and empirical observations. Oikos, *91,* 195–203.

Emmerson M. C., M. Solan, C. Emes, D. M. Paterson and D. Raffaelli. 2001. Consistent patterns and the idiosynchratic effects of biodiversity in marine ecosystems. Nature, *411,* 73–77.

Gerino, M and G. Stora. 1991. Analyse quantitative In vitro de la bioturbation induite par la polychaete Nereis diversicolor. C. R. Acad. Sc. Paris, (ser. 3), *313,* 489–494.

Gilbert F., R. C. Aller and S. Hulth. 2003. The influence of macrofaunal burrow spacing and diffusive scaling on sedimentary nitrification and denitrification: An experimental simulation and model approach. J. Mar. Res., *61,* 101–125.

Gilbert F., S. Hulth, V. Grossi, J-C. Poggiale, G. Desrosiers, R. Rosenberg, M. Gerino, F. François-Carcaillet, E. Michaud and G. Stora. 2007. Sediment reworking activity rates and

patterns in some marine benthic species from the Gullmar Fjord (Western Sweden). Importance of faunal biovolume. J. Exp. Mar. Biol. Ecol., *348,* 133–144.

Graf, G., W. Bengtsson, U. Diesner, R. Schultz and H. Theede. 1982. Benthic response to sedimentation of a spring phytoplanton bloom: process and budget. Mar. Biol., *67,* 201–208.

Grenz, C., J. E. Cloern, S. W. Hager and B. E. Cole. 2000. Dynamics of nutrient cycling and related benthic nutrient and oxygen fluxes during a spring phytoplanton bloom in south San Fransisco Bay (USA). Mar. Ecol. Prog. Ser., *197,* 67–80.

Hall, P. O. J., S. Hulth, G. Hulthe, A. Landen and A. Tenberg. 1996. Benthic nutrient fluxes on a basin-wide scale in the Skagerrak North-Eastern North Sea. J. Sea Res., *351,* 123–137.

Hughes J. and J. Roughgarden. 2000. Species diversity and biomass stability. Am. Nat. *155,* 618–627.

Ieno E., M. Solan, P. Batty and G. Pierce. 2006. How biodiversity affects ecosystem functioning: roles of infaunal species richness, identity and density in the marine benthos. Mar. Ecol. Prog. Ser., *311,* 263–271.

Jorgensen, B. B., R. N. Glud and O. Holby. 2005. Oxygen distribution and bioirrigation in Arctic fjord sediments Svalbard, Barents Sea. Mar. Ecol. Prog. Ser., *292,* 85–95.

Legendre, P. and L. Legendre. 1998. Numerical Ecology, 2nd ed., Elsevier, Amsterdam, 853 pp.

Lewandowski, J., C. Laskov and M. Hupper. 2007. The relationship between Chironomus plumosus burrows and the spatial distribution of pore-water phosphate, iron and ammonium in lake sediments. Freshwater Biol., *52,* 331–343.

Loreau M. and A. Hector. 2001. Partioning selection and complementarity in biodiversity experiments. Nature, *412,* 72–76.

Marinelli, R. L. 1994. Effects of burrow ventilation on activities of a terebellid polychaete and silicate removal from sediment pore waters. Limnol. Oceanogr., *392,* 303–317.

Mermillod-Blondin F., F. François-Carcaillet, and R. Rosenberg. 2005. Biodiversity of benthic invertebrates and organic matter processing in shallow marine sediments: an experimental study. J. Exp. Mar. Biol. Ecol., *326,* 77–88.

Mermillod-Blondin F., M. Gerino, S. Sauvage, and M. Creuzé des Châtelliers. 2004. Influence of nontrophic interactions between benthic invertebrates on river sediment processes: a microcosm study. Can. J. Fish. Aquat. Sci., *61,* 1817–1831.

Mermillod-Blondin F., S. Marie, G. Desrosiers, B. Long, L. de Montety L, E. Michaud and G. Stora. 2003. Assessment of the spatial variability of intertidal benthic communities by axial tomodensitometry: importance of fine-scale heterogeneity. J. Exp. Mar. Biol. Ecol., *287,* 193–208.

Michaud, E., G. Desrosiers, B. Long, L. de Montety, J-F. Crémer, E. Pelletier, J. Locat, F. Gilbert, and G. Stora. 2003. Use of axial tomography to follow temporal changes of benthic communities in an unstable sedimentary environment (baie des Ha! Ha!, Saguenay fjord). J. Exp. Mar. Biol. Ecol., *285–286,* 265–282.

Michaud E, G. Desrosiers, F. Mermillod-Blondin, B. Sundby and G. Stora. 2005. The functional group approach to bioturbation: The effects of biodiffusers and gallery-diffusers of the *Macoma balthica* community on sediment oxygen uptake. J. Exp. Mar. Biol. Ecol., *326,* 77–88.

—— 2006. The functional group approach to bioturbation: II. The effects of the *Macoma balthica* community on fluxes of nutrients and dissolved organic carbon across the sediment-water interface. J. Exp. Mar. Biol. Ecol., *337,* 178–189.

Miron, G. and G. Desrosiers. 1990. Distribution and population structures of two estuarine polychaetes in the St. Lawrence Estuary, with special reference to environmental factors. Mar. Biol., *105,* 297–306.

Miron, G., G. Desrosiers, C. Retière and R. Lambert. 1991. Évolution spatio-temporelle du réseau de galeries chez le polychète *N. virens* en relation avec la densité. Can. J. Zool., *69,* 39–42.

Norling, K., R. Rosenberg, S. Hulth, A. Gremare and E. Bonsdorff. 2007. Importance of functional

biodiversity and species-specific traits of benthic fauna for ecosystems functions in marine sediments. Mar. Ecol. Prog. Ser., *332,* 11–23.

Rhoads, D. C. and D. G. Young. 1970. The influence of deposit feeding organisms on sediment stability and community trophic structure. J. Mar. Res., *28,* 150–178.

Riaux-Gobin C. and B. Klein. 1993. Microphytobenthic biomass measurement using HPLC and conventional pigment analysis, *in* Handbook of Methods in Aquatic Microbial Ecology, P. F. Kemp, B. F. Sherr, E. B. Sherr and J. J. Cole, eds., Lewis Publishers Inc., Boca Raton, 369–376.

Rosenberg, R. 2001. Marine benthic faunal successional stages and related sedimentary activities. Sci. Mar., *652,* 107–119.

Rosenberg, R. E. Davey, J. Gunnarsson, K. Norling and M. Frank. 2007. Application of computer-aided tomography to visualize and quantify biogenic structures in marine sediments. Mar. Ecol. Prog. Ser., *331,* 23–34.

Schaffner, L. C. 1990. Small-scale organism distributions and patterns of species diversity: evidence for positive interactions in an estuarine benthic community. Mar. Ecol. Prog. Ser., *61,* 107–117.

Seitzinger, S. P., J. Harrison, J. Bohlke, A. Bouwman, R. Lowrance, B. Peterson, C. Tobias and G. Van Drecht. 2006. Denitrification across landscapes and waterscapes: a synthesis. Ecol. Appl., *16,* 2064–2090.

Solan M. and R. Kennedy. 2000. Observation and quantification of in situ animal-sediment relations using time-lapse sediment profile imagery t-SPI. Mar. Ecol. Prog. Ser., *228,* 179–191.

Solan M., B. J. Cardinale, A. L. Downing, K. A. M. Engelhardt, J. L. Ruesink and D. S. Srivastava. 2004. Extinction and Ecosystem Function in Marine Benthos. Science, *306,* 1177–1180.

Solorzano, L. 1969. Determination of ammonia in natural waters by the phenol-hypochlorite method. Limnol. Oceanogr., *14,* 799–801.

Strickland, J. D. and T. R. Parsons. 1978. A Practical Handbook of Sea Water Analysis, 2nd ed., Ottawa, Canada, Fish. Res. Bd. Can. Bull., 311 pp.

Sun, M.-Y., C. Lee and R. C. Aller. 1993. Anoxic and oxic degradation of ^{14}C-labeled chloropigments and a ^{14}C-labeled diatom in Long Island Sound sediments. Limnol. Oceanogr., *38,* 1438–1451.

Sun, M.-Y., R. C. Aller, C. Lee and S. G. Wakeham. 2002. Effects of oxygen and redox oscillation on degradation of cell-associated lipids in surficial marine sediments. Geochim. Cosmochim. Acta, *66,* 2003–2012.

Sundby, B., C. Gobeil, N. Silverberg and A. Mucci. 1992. The phosphorus cycle in coastal marine sediments. Limnol. Oceanogr., *37,* 1129–1145.

Waldbusser G. and R. L. Marinelli. 2006. Macrofaunal modification of porewater advection: role of species function, species interaction, and kinetics. Mar. Ecol. Prog. Ser., *311,* 217–231.

Waldbusser G., R. Marinelli, R. B. Whitlatch and P. T. Visscher. 2004. The effects of infaunal biodiversity on biogeochemistry of coastal marine sediments. Limnol. Oceanogr., *495,* 1482–1492.

Widdicombe, S., M. C. Austen, Kendall, R. M. Warwick and M. B. Jones. 2000. Bioturbation as a mechanism for setting and maintaining levels of diversity in subtidal macrobenthic communities. Hydrobiologia, *440,* 369–377.

Woodin, S. 1978. Refuge, disturbance, and community structure: marine soft-bottom example. Ecol., *34,* 25–41.

Zar J. H. 1998. Biostatistical Analysis, Prentice-Hall, NJ, 664 pp.

Zwarts, L. and A. M. Blomert. 1992. Why knot *Calidris canutus* take medium-sized *Macoma balthica* when six prey species are available. Mar. Ecol. Prog. Ser., *83,* 113–128.

Received: *25 July, 2008;* revised: *7 January, 2009.*